Probing carrier dynamics in implanted and annealed polycrystalline silicon thin films using white light

Emmanouil Lioudakis and Andreas Othonos[a)]
Research Center of Ultrafast Science, Department of Physics, University of Cyprus, P.O. Box 20537, 1678 Nicosia, Cyprus

A. G. Nassiopoulou
IMEL/NCSR Demokritos, P.O. Box 60228, 15310, Aghia Paraskevi, Athens 15310, Greece

(Received 4 October 2005; accepted 23 March 2006; published online 3 May 2006)

Polycrystalline silicon thin film samples implanted and annealed at various temperatures have been studied using ultrafast laser pulse excitation. Nondegenerate pump-probe technique has been utilized to investigate carrier dynamics in the highly implanted samples at a relatively small fluence. A model based on two coupled differential equations has been used to fit the experimental data, giving a simple but adequate picture of the dynamics of this system. Basic sample parameters such as carrier trapping times, diffusion coefficient, and penetration depths have been extracted, providing a dependence on the annealing temperature for the samples under investigation. © *2006 American Institute of Physics*. [DOI: 10.1063/1.2200745]

The dynamics of optically excited electron-hole plasmas in semiconductors have been investigated extensively over the past two decades.[1] The available technology of femtosecond lasers source has let to an enormous progress in understanding the basic relaxation mechanisms of carriers in semiconductors.[2,3] The recent requirement of miniaturization of semiconductor devices into the nanometer regime and the complexity of the devices has placed a great deal of emphasis in the clear understanding of the carrier dynamics on shorter time scales and over broader span of energies. Key processes such as ion implantation and subsequent annealing for silicon based devices have a tremendous impact on the carrier dynamics and energy relaxation in these materials.[4–6] Clearly, obtaining a good understanding of these processes and their effect on carrier dynamics and energy relaxation in these materials is vital for further development in microelectronics. The demand for high-speed optoelectronic devices with ultrafast response has given a renewed interest in this area.[7,8]

Following optical excitation, electrons and holes undergo spatial and temporal evolutions with characteristic times which depend on the various relaxation processes.[1–3] Initially, the excitation energy is transferred entirely to the carriers, leading to the creation of nonequilibrium carrier densities with specific momentum states and elevated carrier temperatures. As the system evolves towards equilibrium, there is momentum and energy relaxations. Momentum relaxation occurs on a femtosecond time scale via elastic and inelastic scatterings. On the same time scale carrier-carrier scatterings of the electrons (holes) results in Coulomb thermalization and allows the electron (hole) system to be described by a Fermi-Dirac distribution. Similarly electron-hole scattering eventually brings the two distributions into thermal equilibrium. Eventually energy relaxation of these carriers results in transferring energy to the lattice. The dynamics of these photogenerated carriers can be monitored directly using time resolved reflectivity measurements.[1]

Here, we report on ultrafast transient white-light reflectivity measurements on highly implanted and annealed polycrystalline silicon samples. The source of short pulses consists of a self-mode-locked Ti:sapphire oscillator generating 100 fs pulses at 800 nm. A regenerative amplifier system is used to amplify the pulses to approximately 1 mJ at a repetition rate of 1 kHz. The ultrashort pulses are used in a pump-probe setup where the pump beam is frequency doubled at 400 nm using a nonlinear crystal [beta barium borate (BBO)]. A small part of the fundamental energy is used to generate a supercontinuum spectrum by focusing the beam on a thin sapphire plate. The white light generated is used in a noncollinear geometry in a pump-probe configuration to carry out transient reflectivity measurements. Narrow bandpass filters are utilized in front of the detector to select the wavelength. The temporal variation in the index of refraction was monitored as a change in the reflectivity, which was a direct measure of the photoexcited carrier dynamics within the probing region. Observation of the short and long time behaviors in these samples has been investigated.

The samples used in these experiments were 1 μm polycrystalline silicon films on quartz implanted with arsenic ions at doses of 2×10^{16} ions/cm^2 and implantation energy $E=100$ keV. The growth of the polycrystalline films was accomplished using low pressure chemical vapor deposition of silicon from silane at a temperature of 610 °C and a pressure of 300 mTorr. After implantation, the samples were then thermally annealed in a conventional furnace at various temperatures up to 1100 °C for 1 h in an inert nitrogen atmosphere.

In what follows we will report on transient reflectivity measurements obtained with a fluence of ~5 mJ/cm^2 at 400 nm. Reflectivity measurements were taken at several probing wavelengths covering a range from 400 to 500 nm. Figure 1 shows reflectivity measurements for the nonannealed and annealed samples at 500 nm. The graphs show both short and long time behaviors following ultrafast pulse excitation. On the short time scale we notice a pulse-width-limited drop in the reflectivity for all the samples. Following this initial drop, all the samples appear to have different temporal recoveries of the reflectivity. The nonannealed sample

[a)]Author to whom correspondence should be addressed; electronic mail: othonos@ucy.ac.cy

 © 2006 American Institute of Physics
Downloaded 30 May 2010 to 194.42.23.188. Redistribution subject to AIP license or copyright; see http://apl.aip.org/apl/copyright.jsp

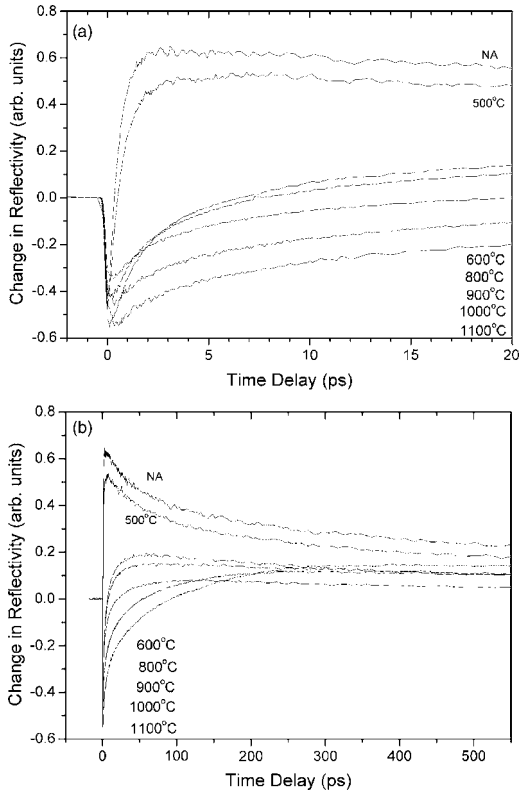

FIG. 1. Transient reflectivity responses of the ion-implanted nonannealed and annealed polycrystalline silicon samples probed at 500 nm. (a) Short time and (b) long time scales.

appears to have the fastest recovery from the negative reflectivity following ultrashort pulse excitation. This recovery time was estimated to be approximately 0.6 ps. Similar behavior is observed for the samples annealed at low temperatures up to 500 °C. A noticeable change is observed for samples annealed at temperatures higher than 600 °C. The recovery time from the maximum negative change in reflectivity increases with increasing annealing temperature.

The transient reflectivity on the long time scale can be separated into two distinct groups, corresponding to the low and high temperature annealed samples. In the low temperature annealed samples, the negative change in reflectivity and the fast recovery to a maximum positive change are followed by a slow recovery toward equilibrium over several hundred picoseconds. On the other hand, with increasing annealing temperature, the recovery to the positive reflectivity occurs at a much lower value with again a slow recovery toward equilibrium.

The ultrafast recovery behavior of the nonannealed and annealed at 500 °C samples, which is exponential, may be attributed to the ion-induced traps in the polycrystalline samples, following implantation with arsenic at a high dose. It is important to point out that there are distinct differences in the recovery of the reflectivity between the nonannealed and annealed samples at 500 °C.

The observed recovery and subsequent temporal reflectivity behavior may be understood using a relatively simple model. Following short pulse excitation with above band gap photons, a large carrier density is generated. These carriers will result in changes in the index of refraction of the material, which will result in changes in reflectivity. Initially, the induced carriers will result in a negative change in reflectivity, due to free carriers (Drude expression) and band filling. With relaxation of the carriers and subsequent energy transfer to the lattice, there will be an increase in the film temperature, resulting in a positive increase of the index of refraction. The combination of the two contributions results in the rather complex behavior observed for the implanted and annealed samples.

To describe the carrier dynamics, we use two coupled differential equations, one for the carrier density and one for lattice temperature. These equations include diffusion and recombination of carriers. In this model, we are assuming that after the carriers are captured by the ion-induced traps, they will eventually transfer their energy to the lattice. Although the effect of band gap renormalization is difficult to be quantified, intensity measurements carried out in these samples suggest that this effect may be neglected under our experimental conditions. The boundary conditions used in this model correspond to the front and back surfaces of the sample,

$$\frac{\partial N(z,t)}{\partial t} = D_N \frac{\partial^2 N}{\partial z^2} - \frac{N}{\tau_{\text{trap}}}, \quad N(z,0) = N_0 \exp(-\alpha z),$$

$$\left.\frac{\partial N}{\partial z}\right|_{z=0} = \frac{S}{D_N} N(0,t), \quad N(\infty,t) = 0,$$

$$\frac{\partial \Delta T(z,t)}{\partial t} = D_L \frac{\partial^2 \Delta T}{\partial z^2} + \frac{E_g}{\rho C} \frac{N}{\tau_{\text{eff}}},$$

$$\Delta T(z,0) = \Delta T_0 \exp(-\alpha z),$$

$$\left.\frac{\partial \Delta T}{\partial z}\right|_{z=0} = -\frac{E_g}{\rho C} \frac{S}{D_N} N(0,t), \quad \Delta T(\infty,t) = 0.$$

N corresponds to the carrier density, D_N is the ambipolar diffusion coefficient, τ_{trap} is the carrier trapping time (this is the time required for the carriers to be captured by the traps), τ_{eff} is the effective carrier lifetime given by $1/\tau_{\text{eff}} = 1/\tau_L + 1/\tau_{\text{e-h}}$, where τ_L is the trapped carrier lifetime and $\tau_{\text{e-h}}$ is the normal electron-hole recombination time, S is the surface recombination, and D_L is the thermal diffusivity. Auger recombination is considered negligible for the carrier densities involved in these experiments; therefore it is not included in the above equations.

The above set of equations may be solved analytically as described in Ref. 9. Given that the index of refraction depends on the carrier density (free carriers and band filling) and lattice temperature, the induced change in reflectivity may be estimated.[6,10] Using the experimental parameters of this work we have been able to perform fits to our experimental data. Parameters that were varied and optimized for the best fit to the results were ambipolar diffusion coefficient, carrier trapping time, absorption coefficient, thermal diffusivity, and effective carrier lifetime. All other parameters were assumed to be close to the values of silicon.[11]

For illustration purposes Fig. 2 shows experimental data probed with 450 nm white light for three samples, compared with the fitting results based on the above described model. Although in these graphs we show relatively short time scales, good agreement with the experimental data has also been achieved on long time scales. It is interesting to note that the nonannealed sample shown in the inset of Fig. 2 has the fastest recovery following short pulse excitation. The best fit parameters for these data were carrier trapping time

Downloaded 30 May 2010 to 194.42.23.188. Redistribution subject to AIP license or copyright; see http://apl.aip.org/apl/copyright.jsp

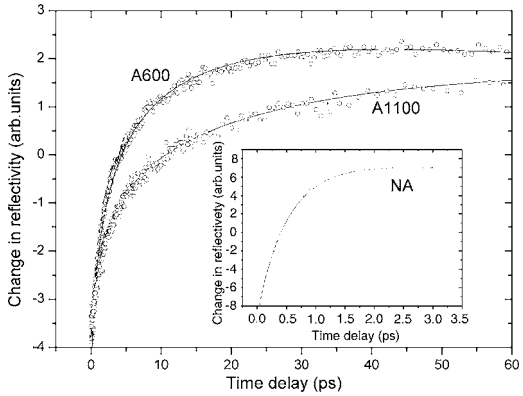

FIG. 2. Fittings of the experimental data at various annealing temperatures at the 450 nm probing wavelength. Fittings are based on the coupled differential equations describing the carrier and lattice dynamics following ultrafast pulse excitation.

of ~0.6 ps, ambipolar diffusion of 1 cm^2/s, absorption coefficient of $2.1\times10^5\ cm^{-1}$, thermal diffusivity of 0.86 cm^2/s, and effective carrier lifetime of 0.8 ns. With increasing annealing temperature, the carrier trapping time increases dramatically to 50 ps for the 600 °C annealed sample and to 140 ps for the sample annealed at the highest temperature (11000 °C). Furthermore, the effective carrier lifetime increases with increasing annealing temperature. Parameters such as ambipolar diffusion and absorption coefficient also change with increasing annealing temperature. A more complete picture of the behavior of these key parameters following annealing of the samples is shown in Fig. 3.

Figure 3(a) shows the absorption coefficient for various probing wavelengths as a function of annealing temperature. Clearly evident is the monotonically decreasing absorption coefficient value with increasing annealing temperature. Furthermore, the higher values of absorption coefficient, which are observed for the short probing wavelengths, are in agreement with the extracted values from ellipsometry measurements[12] performed on the same set of samples. In Fig. 3(b) we present the fitted trapping time obtained from simulations. Here, the behavior is rather complex. For the nonannealed and the annealed up to 500 °C samples, the carrier trapping time is estimated to be approximately 0.6 ps. This is expected due to the high density of traps generated in the sample during ion implantation. There is a sharp increase in the carrier trapping time at 600 °C due to the removal of the traps within the probing region of the sample. The carrier trapping time continues to increase by increasing the annealing temperature, as expected, due to gradual removal of the traps from the samples. The variation due to the probing wavelength is simply due to the variation of the probing penetration depth. At shorter wavelengths, the penetration depth is shorter and closer to the surface where most of the implantation damage occurs, resulting in the high density of traps. As a result the carrier trapping time is shorter for shorter wavelengths. Finally, Fig. 3(c) shows the fitted ambipolar diffusion coefficients as a function of annealing temperature. We note that the coefficient is very small for the nonannealed and annealed up to 500 °C samples. There is a sharp increase of the value of this coefficient, reaching the value corresponding to that of crystalline silicon at the highest annealing temperature.

In conclusion we have utilized ultrafast temporal reflectivity white-light technique in conjunction with a model of coupled differential equations to investigate the dynamics of implantation and annealing on key optical parameters of polycrystalline silicon thin film samples.

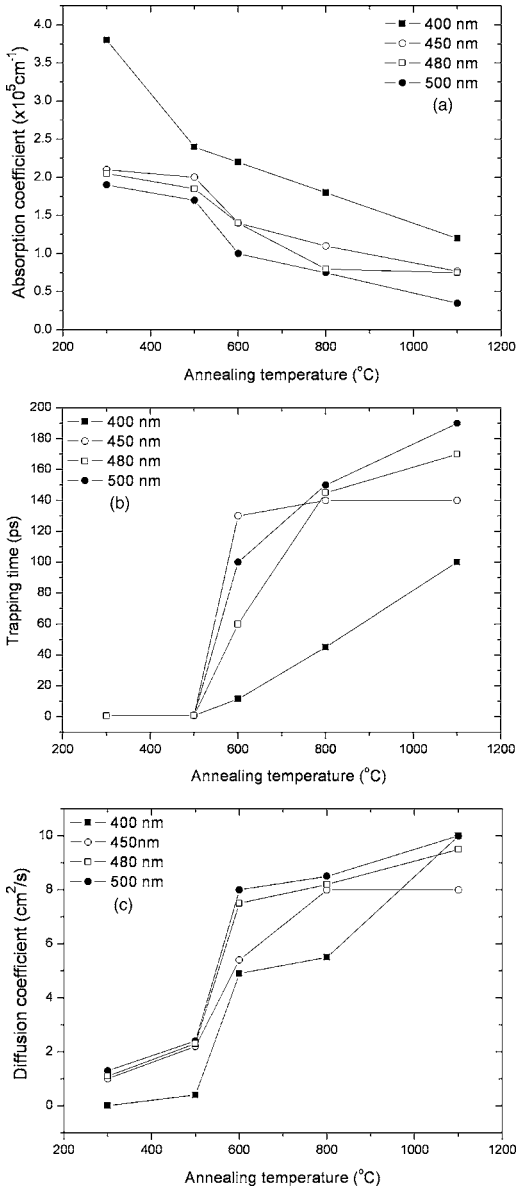

FIG. 3. Plots of the fitted parameter for (a) the absorption coefficient, (b) carrier trapping time, and (c) diffusion coefficient as a function of the annealing temperature.

[1] J. Shah, *Ultrafast Spectroscopy of Semiconductors and Semiconductor Nanostructures* (Springer, New York, 1999).
[2] Ellen J. Yoffa, Phys. Rev. B **21**, 2415 (1980).
[3] A. Othonos, J. Appl. Phys. **83**, 1789 (1998).
[4] F. E. Doany, D. Grischkowsky, and C. C. Chi, Appl. Phys. Lett. **50**, 460 (1987).
[5] Albert Chin, K. Y. Lee, and B. C. Lin, Appl. Phys. Lett. **69**, 653 (1996).
[6] A. Othonos and C. Christofides, Phys. Rev. B **66**, 085206 (2002).
[7] A. J. Sabbah and D. M. Riffe, Phys. Rev. B **66**, 165217 (2002).
[8] K. E. Myers, Q. Wang, and S. L. Dexheimer, Phys. Rev. B **64**, 161309 (2001).
[9] Takayuki Tanaka, Akira Harata, and Tsuguo Sawada, J. Appl. Phys. **82**, 4033 (1997).
[10] M. C. Downer and C. V. Shank, Phys. Rev. Lett. **56**, 761 (1986).
[11] *Physics of Group II-IV Elements and I-VII Compound*, Landolt-Bornstein, New Series, Group III, Vol. 17, Pt. B, edited by O. Madelung, M. Schulz, and H. Weiss (Springer, New York, 1982).
[12] E. Lioudakis, A. G. Nassiopoulou, and A. Othonos, Thin Solid Films **496**, 235 (2006).

Downloaded 30 May 2010 to 194.42.23.188. Redistribution subject to AIP license or copyright; see http://apl.aip.org/apl/copyright.jsp